https://doi.org/10.5194/egusphere-2024-2144
Preprint. Discussion started: 30 July 2024

A long-term drought reconstruction based on oxygen isotope tree ring data

Viorica Nagavciuc [1,2*] Gerhard Helle [3], Maria Rădoane [2], Cătălin-Constantin Roibu [2], Mihai-Gabriel Cotos [2] and Monica Ionita[1,2*]

[1] Alfred Wegener Institute for Polar and Marine Research, Bremerhaven 27570, Germany

[2] Forest Biometrics Laboratory – Faculty of Forestry, "Stefan cel Mare" University of Suceava, Universității Street No. 13, Suceava 720229, Romania

[3] German Research Centre for Geosciences GFZ, 4.3 Climate Dynamics and Landscape Evolution, Telegrafenberg, 14473 Potsdam, Germany

Correspondence to: Monica Ionita (Monica.Ionita@awi.de); Viorica Nagavciuc (nagavciuc.viorica@gmail.com);

Abstract. This study investigates the relationship between oxygen isotope ratios ($\delta^{18}O$) in oak tree ring cellulose and past drought variability in Letea Forest, Romania. A $\delta^{18}O$ site chronology spanning 1803-2020 was compiled from seven individual time series. $\delta^{18}O$ values exhibited a significant negative correlation with moisture-related variables (cloud cover, relative humidity and precipitation) and a positive correlation with temperature and sunshine duration. This confirms that $\delta^{18}O$ from tree rings can be a good proxy for moisture availability. The strongest correlation was found between $\delta^{18}O$ and the August Standardized Precipitation Evapotranspiration Index for an accumulation period of 9-months (SPEI9) for central and eastern Europe. This highlights SPEI9 as a superior indicator of drought compared to individual parameters like temperature or precipitation. Using a linear regression model, we reconstructed August SPEI9 variability for the past 200 years. The reconstruction captured interannual and decadal variations, with distinct wet and dry periods. Analysis of large-scale atmospheric circulation patterns revealed a link between high $\delta^{18}O$ values (indicating dry conditions) and a high-pressure system over the North Atlantic. Conversely, low $\delta^{18}O$ values (indicating wet conditions) corresponded to negative pressure anomalies over Europe. Moreover, extreme values of $\delta^{18}O$ are also associated with the prevalence of a hemispheric teleconnection pattern, namely wave number 4. This $\delta^{18}O$ chronology and the corresponding August SPEI9 reconstruction offer valuable tools for understanding past climate variability and its relationship with large-scale atmospheric and oceanic circulation patterns.

Keywords

Danube River Delta, Romania, oak tree rings, drought reconstruction, August SPEI9, large-scale atmospheric circulation

https://doi.org/10.5194/egusphere-2024-2144
Preprint. Discussion started: 30 July 2024

1. Introduction

Droughts are a recurring natural phenomenon with significant environmental and socio-economic impacts (Kreibich et al., 2022). Understanding past drought occurrences and their frequency, intensity, and spatial extent is crucial for predicting future occurrences, and trends, mitigating risk, and adapting water management strategies, particularly as climate change intensifies (IPCC, 2021; Van Loon et al., 2024).

Romania, situated in southeastern Europe, is particularly vulnerable to droughts due to its geographical location and complex climatic dynamics (Nagavciuc et al., 2022b). The country experiences a wide range of climatic conditions, with distinct variations in precipitation patterns across different regions. This inherent variability, coupled with the projected increase in global temperature and altered circulation patterns, raises concerns about the potential for more frequent and intense droughts in the future (Ionita et al., 2021, 2022; Ionita and Nagavciuc, 2021).

While instrumental records provide valuable insights into recent droughts, they only span a rather short timeframe, making it challenging to assess long-term drought variability and identify potential patterns. In this context, tree rings emerge as powerful archives of past environmental conditions, acting as biological dataloggers, recording environmental changes in the arboreal system year after year throughout the lifespan of a tree. Analyzing the variations in their width, density, and isotopic compositions provides valuable insights into historical climatic conditions, including temperature, precipitation, and drought variability (Leavitt, 2010; Nagavciuc et al., 2020; Schweingruber, 1988; Siegwolf et al., 2022).

Among the various tree-ring proxies, stable oxygen isotopes ($\delta^{18}O$) have proven to be a powerful tool for reconstructing past drought occurrences in very different environments across various climate zones and altitudes (Baker et al., 2022; Feng et al., 2022; Nagavciuc et al., 2019b, 2024; Pumijumnong et al., 2020; Saurer et al., 2012; Van der Sleen et al., 2015). The $\delta^{18}O$ values in tree-ring cellulose reflect the ratio of heavier (^{18}O) to lighter (^{16}O) oxygen isotopes incorporated during cellulose formation. This ratio is primarily influenced by the availability of soil water, making it highly sensitive to drought stress (Allen et al., 2018; Gessler et al., 2022; McCarroll and Loader, 2004; Siegwolf et al., 2022).

Trees primarily take up water from the soil, and this soil water is replenished by precipitation. At the leaf surface, water undergoes evapotranspiration. Lighter oxygen-16 isotopes evaporate more readily, leaving the remaining leaf water enriched in heavier oxygen-18. The degree of enrichment generally depends on the leaf-to-air vapor pressure difference which is predominantly connected to air temperature and humidity. Drier conditions enhance this evapotranspiration, further increasing the oxygen-18 concentration of leaf water (Gessler et al., 2014; Roden et al., 2000). Therefore, analyzing the $\delta^{18}O$ values in tree rings provides a direct proxy for past drought events (Freund et al., 2023; Gagen et al., 2022; Loader et al., 2020; McCarroll and Loader, 2004; Nagavciuc et al., 2024; Young et al., 2015).

A strong relationship between $\delta^{18}O$ in oak trees and water availability (Robertson et al., 1995; Young et al., 2015), corroborated with the availability of continuous records with yearly resolution spanning several centuries, and the widespread distribution of centuries-old trees oak, make the $\delta^{18}O$ values in oak tree-ring cellulose from the Danube Delta, Romania the ideal candidate for long-term drought reconstruction. They have the potential to significantly contribute to a better understanding of past drought events beyond the limitations of instrumental data, providing a better picture of past hydroclimatic conditions of the Danube River catchment integrating over large parts of the country and south-eastern central Europe.

This research aims to reconstruct long-term drought variability over the last 200 years in the southern-eastern part of Romania using stable oxygen isotopes ($\delta^{18}O$) extracted from oak tree rings from Letea Forest, Danube Delta (29°34'51"E

https://doi.org/10.5194/egusphere-2024-2144
Preprint. Discussion started: 30 July 2024

45°18'10"N). This study strives to address the following specific objectives: i) to establish an annually resolved $\delta^{18}O$ chronology compiled from individual sequences from oak trees (*Quercus Sp.*) sampled at the Letea Forest, Danube Delta Romania; ii) to develop a robust statistical model linking $\delta^{18}O$ values to instrumental drought indices (Standardized Precipitation Evapotranspiration Index, SPEI), allowing for the reconstruction of past drought variability; iii) to analyze the spatial and temporal patterns of reconstructed drought occurrences, identifying periods of severe droughts that affected the upstream Danube River catchment and iv) to investigate potential linkages between reconstructed drought events and large-scale atmospheric circulation patterns, providing insights into the underlying mechanisms of drought in the region.

2. Methods

2.1 Study Site

The Danube Delta has remarkable biodiversity and a special place in the flora of the Delta is covered by the Letea Forest, one of the oldest natural reserves in Romania and the northernmost subtropical forest in the world (Abdelazim and Diaconu, 2022). The Letea Forest is located in the northeast part of the Danube Delta, between the Chilia and Sulina branches of the Danube River. The Letea Forest (5246,8 ha) has been protected since 1930 and, from 1938 onwards it was declared a strictly protected area (2825 ha) (Administraţia Rezervaţiei Biosferei Delta Dunării, 2022). It developed in the form of narrow strips, sometimes several dozen meters long, called "hasmacuri" in the spaces between the sand dunes, and is represented by mixed oaks and other broadleaves tree species (e.g. *Quercus, Fraxinus, Ulmus*), with some very particular elements of species with voluble stem (e.g. *Periploca graeca, Vitis sylvestris, Humulus lupus, Clematis vitalba*) (Administraţia Rezervaţiei Biosferei Delta Dunării, 2022; info-delta, 2023). The climate is mainly influenced by the proximity of the Black Sea, with warm summers and cold winters. The average annual temperature (i.e., climatological period 1971 - 2000), at Sulina meteorological station (29°39'48"E 45°9'13"N), (i.e., the closest meteorological station to our sampling site), is around 11.18 °C, with July as the warmest month (~22.16 ◦C) and January as the coldest one (~0.43 ◦C). The rainfall is around 278 mm/year, with January as the driest month (~15.4 mm/month) and June as the wettest month (~34 mm/month), while the month with the highest relative humidity is December (88.72 %), and the month with the lowest relative humidity is May (78.14 %) (Figure 1).

2.2 $\delta^{18}O$ tree-ring chronology

A field campaign to Letea Forest was organized in May 2021, when 42 increment cores (one core per tree) were extracted using a 5 mm diameter increment borer from 40 living dominant trees with ages between 114 and 396 years, following standard dendrochronological sampling methods (Schweingruber, 1988). All samples were cut using the WSL core microtome (Gärtner and Nievergelt, 2010), and scanned using a flatbaden scanner Epson 11000XL with a true resolution of 1500 dpi. The scanned images were measured using the CooRecorder v.9.31 software with a precision of 0.01 mm (Cybis Elektronik, 2010). The obtained time series were cross-dated using CDendro (Cybis Elektronik, 2010) and checked for the missing rings using COFECHA software (Holmes, 1983).

The stable isotope analyses were performed for the 1803-2020 period. Latwood rings of seven selected cores were dissected manually with a scalpel to obtain annual resolution before measurement of each ring individually (no pooling). Holocellulose was extracted from latewood(??) using the Jayme-Wise two-step base-acid methodology and setup as described by (Helle et al., 2022): sodium hydroxide for extractives removal followed by acidified sodium chlorite to eliminate lignins following extraction, samples were washed thoroughly with milli-Q water, homogenized (ultrasonic sonode device for Eppendorf sample vials) and then freeze-dried for 48 hours (Laumer et al., 2009) resultant homogenized cellulose was weighed (160-200µg) and packed in silver capsules for stable oxygen isotope analysis. Measurements were completed on an Isotope Ratio Mass Spectrometer Delta V, ThermoFisher Scientific, Bremen, Germany with TC/EA HT pyrolysis device at 1400°C. The samples analyzed are referenced to standard materials from the International Atomic Energy Agency (IAEA-C3, IAEA-CH6, IAEA-

https://doi.org/10.5194/egusphere-2024-2144
Preprint. Discussion started: 30 July 2024

601, and IAEA-602), and checked with secondary standards from Sigma-Aldrich Chemie GmbH, Munich, Germany (Sigma Alpha-Cellulose and Sigma Sucrose) using a two-point normalization method (Paul et al., 2007). Sample replication resulted in reproducibility of better than ± 0.3‰ for the $\delta^{18}O$ values. All isotope values are reported in per mil (‰) relative to the Vienna Standard Mean Ocean Water (VSMOW) (Coplen, 1994), using the traditional δ (delta) notation. The final $\delta^{18}O$ chronology was calculated as the arithmetic mean of the multiple measurements.

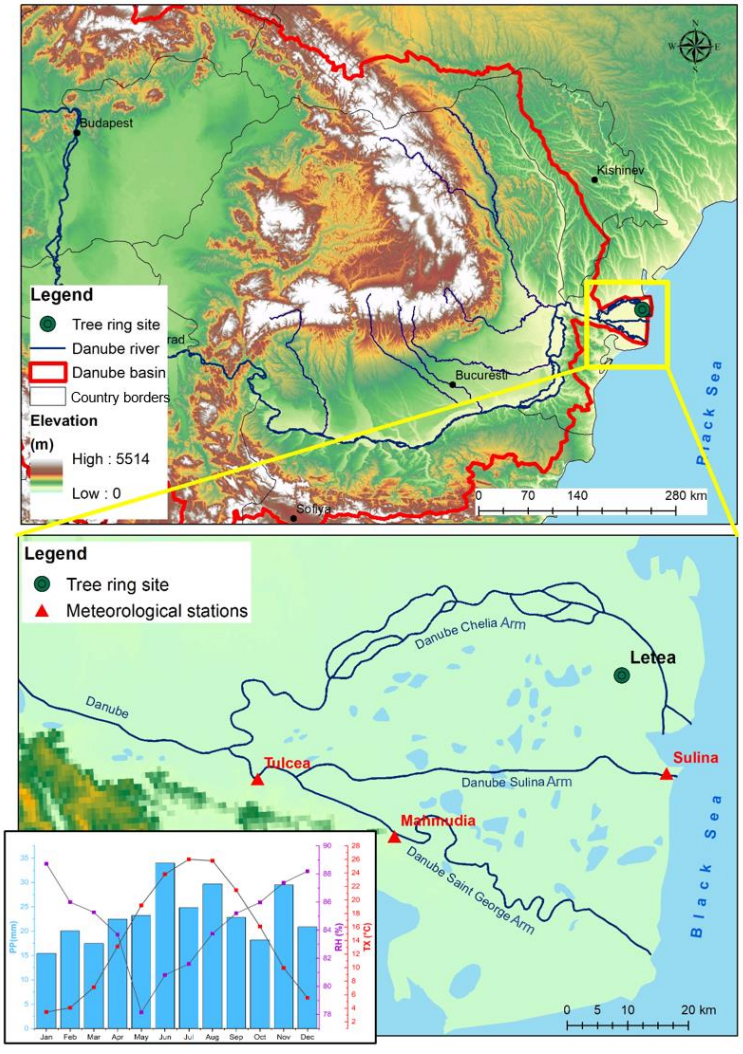

Figure 1. Location of the investigation area. a) the topographic map of Romania showing the sampling site and the eastern Danube River catchment (red line); b) the local map of the Danube Delta with locations of the sampling site (green circle) and climate stations (red triangles). The lower left plot represents the annual variation of the maximum temperature (red dots), precipitation (PPT, blue bars), and relative humidity (violet dots) over the 1971–2000 period at the Sulina meteorological station located ca. 15km south of the study site.

https://doi.org/10.5194/egusphere-2024-2144
Preprint. Discussion started: 30 July 2024

2.3 Hydroclimate data and $\delta^{18}O$ relationship

The hydroclimatic sensitivity of the $\delta^{18}O$ was tested by performing correlation analyses between $\delta^{18}O$ and precipitation, mean temperature, maximum temperature, relative humidity, cloud cover, and sunshine duration using monthly climate data from the Sulina meteorological station. All correlation analyses were performed from January to December, but also for March, April, and May (MAM), June, July, and August (JJA), and from January to August (J-A).

Since the available data from Sulina was constrained to 1961-2013 we performed additional analyses with gridded data obtained from the CRU TS v. 4.04 dataset (Harris et al., 2020), covering the period 1901-2020. Given that the stable oxygen isotopes in tree ring cellulose are sensitive to precipitation and temperature, we also tested the relationship with the drought index, namely with the Standardized Precipitation Evapotranspiration Index (SPEI). To compute the SPEI we used the gridded monthly precipitation (PP), monthly mean air temperature (TT), and potential evapotranspiration (PET). The correlation between $\delta^{18}O$ chronology and the SPEI index was tested for different time scales: one month (SPEI1), three months (SPEI3), six months (SPEI6), nine months (SPEI9), and 12 months (SPEI12), and for different months, from January until the September current year, in order to identify the most suitable period for reconstruction.

The spatial stability of the correlations between our reconstruction and the Standardized Precipitation Evapotranspiration Index (SPEI), was assessed using the SPEI for an accumulation period of 9-months (SPEI9). Calculations were performed using the R-package SPEI (https://cran.r-project.org/web/packages/SPEI/index.html) at a spatial resolution of 0.5° × 0.5°. The relationship between our reconstruction and the large-scale atmospheric circulation has been analyzed using the monthly means of Geopotential Height at 500mb (Z500), zonal wind at 500 mb (U500), and meridional wind at 500mb (V500) and at 200mb (V200) from the Twentieth Century Reanalysis (V3) dataset (2◦ ×2◦ grid, 1837–2015 CE). Sea surface temperature (SST) data was extracted from the ERSST V5 dataset (2° x 2°, 1854 – 2020). These datasets offer extended temporal coverage (~180 years for atmospheric, ~167 years for oceanic) and have been successfully used in paleoclimate studies (Ionita et al., 2021; Nagavciuc et al., 2022a; Roibu et al., 2022).

2.4 Statistical methods and reconstruction model

The spatial stability of the $\delta^{18}O$ – SPEI relationship was tested by using so-called stability maps, a methodology successfully used to examine the stationarity of the long-term relationship in seasonal river forecast(Ionita et al., 2008, 2014, 2018) and dendrochronological studies (Nagavciuc et al., 2019a, 2022a; Roibu et al., 2022).

For drought reconstruction, we used the August SPEI for the accumulation period of nine months (Aug SPEI9) covering the period 1900–2020, over the eastern part of Europe. The reconstruction model was developed using the R packages dplR (Bunn, 2008) and treeclim (Zang and Biondi, 2015), using the linear regression model. The predictive skills of the reconstructed model were tested by using split-period calibration/verification and statistics including the coefficient of determination (R^2), the reduction of error (RE), and the coefficient of efficiency (CE), whereas RE and CE >0 were required (Briffa and Jones, 1992). Additionally, the Durbin–Watson statistic (DW) was used to test the trend in the residuals (Durbin and Watson, 1950). The model calibration was carried out for the 120-year period between 1900 and 2020. The two-equal periods of calibration and verification statistics were performed in two 60-year sub-periods from 1900 to 1960 and from 1961 to 2020.

The number of extreme years in the reconstructed August SPEI9 for the past 200 years was determined by counting the years that fall outside the range of values contained between the 10th percentile (0.1 quantile) and the 90th percentile (0.9 quantile).

https://doi.org/10.5194/egusphere-2024-2144
Preprint. Discussion started: 30 July 2024

The synchronicity of our reconstruction with other reconstructions was tested by analyzing the four previously published reconstructions available in the surrounding area: one August SPEI3 from Eastern Carpathian, Romania (Nagavciuc et al., 2022a), and one September SPEI6 from the Czech Republic (Brázdil et al., 2016), one precipitation reconstruction from the eastern Black Sea Region, Turkey (Akkemik et al., 2005), and one streamflow reconstruction for the Lower Danube River, at Ceatal Izmail hydrometric station (Nagavciuc et al., 2023).

3. Results and Discussions

3.1 Characteristics of Oxygen Isotope Chronology

The $\delta^{18}O$ chronology was developed based on the seven individuals measured $\delta^{18}O$ time series from the Letea Forest, Romania (Figure 1), and covers the 1803 – 2020 period. The $\delta^{18}O$ values of the combined chronology vary around the mean of 27.9 ‰, ranging from 26.1‰ recorded in 1941 to 29.7‰ recorded in 1963 (Figure S3). The first-order autocorrelation for $\delta^{18}O$ data (AC1) is 0.47 and decreases to 0.21 for the second-order autocorrelation (AC2). The mean sample replication for the analyzed period is 7 series, only a smaller replication is available between 1803 and 1813, where the replication reaches 4 series. In confirmation of literature results (Duffy et al., 2019), our $\delta^{18}O$ series show no juvenile effects or common increasing or decreasing trends in the first 140 years of tree age, therefore, we conclude that $\delta^{18}O$ values from oak tree-ring cellulose from Letea Forest can be used for dendroclimatological studies without any detrending procedure.

3.2 Hydro-Climate– $\delta^{18}O$ values relationships

Climate signal strength in the oxygen isotope chronology was evaluated by computing the monthly and seasonal (different combinations of months) Pearson's correlations between the $\delta^{18}O$ values and different climatic parameters available from the Sulina meteorological station for 52 years (1961-2013) (Figure 2). Our results show significant ($p< 0.05$) and negative correlations with cloud cover ($r = -0.54$), precipitation ($r = -0.39$) and relative humidity ($r = -0.46$), and significant and positive correlation with sunshine duration ($r = 0.46$), maximum temperature ($r = 0.44$), mean temperature ($r = 0.39$) and minimum temperature ($r = 0.28$).

The significant correlations between our $\delta^{18}O$ chronology and monthly cloud cover, relative humidity, and precipitation are all negative, while with the sunshine duration and temperature, correlations are positive, which means that the $\delta^{18}O$ variability in oak tree-ring celluloses in the studied area depends primarily on the moisture conditions. Moisture conditions (high cloud cover, relative humidity, precipitation, and low temperatures) determine higher stomatal conductance and a lower transpiration rate which leads to lower $\delta^{18}O$ values in tree-ring cellulose. Conversely, dry climatic conditions (periods of reduced precipitation, low relative humidity, and higher temperatures) determine the reduction of stomatal conductance and higher transpiration rate, which leads to higher $\delta^{18}O$ values in their cellulose (McCarroll and Loader, 2004; Siegwolf et al., 2022).

We have tested also the relationship between $\delta^{18}O$ values and the SPEI at Sulina station, with different accumulation periods (e.g., 1, 3, 6, 9 and 12-months). The obtained results reveal that the $\delta^{18}O$ values are significant (95% significance level) and negatively correlated with all tested SPEI drought indices from the summer months. Correlation coefficients were found lower for shorter time scales (e.g. SPEI1, SPEI3), but they increased for longer time scales (SPEI 6, SPEI9) (Figure 3). The Letea $\delta^{18}O$ Chronology is significantly and negatively correlated with Jul SPEI1 ($r = -0.42$, $p<0.05$), with Aug SPEI3 ($r = -0.57$, $p<0.05$), with August SPEI6 ($r = -0.60$, $p<0.05$), with Aug SPEI12 ($r = -0.57$, $p<0.05$), and the highest correlation coefficient was obtained for Aug SPEI9 ($r = -0.63$, $p<0.05$). The obtained significant correlations imply that the $\delta^{18}O$ values in the oak tree-ring cellulose from Letea Forest are constrained by water availability. The higher correlation with the drought index compared to temperature or precipitation suggests that the SPEI is a more effective indicator of moisture levels than using

https://doi.org/10.5194/egusphere-2024-2144
Preprint. Discussion started: 30 July 2024

precipitation or temperature alone, as it considers both precipitation and temperature through evapotranspirative demand. The obtained higher correlation for longer time scales (e.g., SPEI9), compared to shorter time scales (e.g., SPEI1), indicates that the $\delta^{18}O$ values in this area tend to respond more significantly to drought over extended periods (Gessler et al., 2014; Roden et al., 2000).

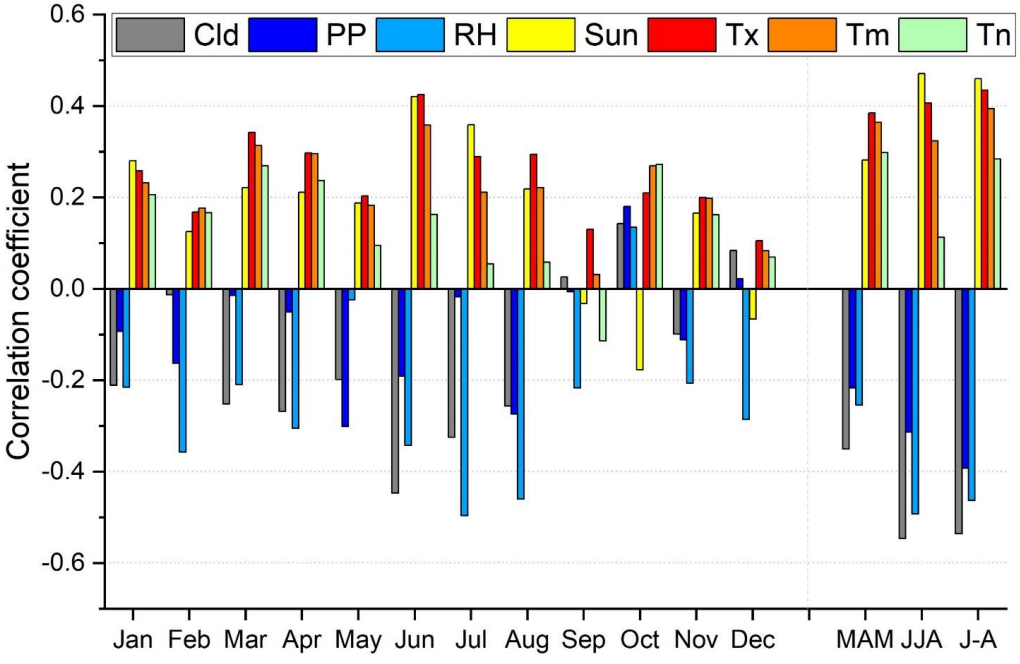

Figure 2. The correlation coefficients of $\delta^{18}O$ chronology from Letea Forest with monthly climate data (cloud cover – Cld, precipitation – PP, relative humidity – RH, sunshine duration – Sun, maximum temperature – Tx, mean temperature – Tm, minimum temperature – Tn) from Sulina meteorological station. Correlation analyses were performed from January to December, but also for March, April, and May (MAM), June, July, and August (JJA), and from January to August (J-A).

The spatio–temporal stability of hydroclimatic signals was tested by applying the stability maps approach between the $\delta^{18}O$ values and the gridded mean temperature (TT), precipitation (PP), and SPEI9 data over the period 1901–2020, based on the CRU TS v. 4.04 data (Harris et al., 2020). Stability map analyses with precipitation show a significant and stable correlation in summer over the eastern part of Romania, the Republic of Moldova, and the central part of Ukraine (Figure S1). The results obtained for stability maps with temperature show a significant and stable correlation in April over central and northern Europe, in June over south-western Europe, in August over Hungary and Slovakia, in March-April-May over central Europe, and in June-July-August over the southern part of France (Figure S2).

Stability maps for $\delta^{18}O$ values and SPEI9 data reveal a significant and stable correlation starting February until October, including spring (March-April-May) and summer (June-July-August). In February and March, the correlation is significant and stable over a small region in the southeastern part of Romania and the southern part of the Republic of Moldova, the region

https://doi.org/10.5194/egusphere-2024-2144
Preprint. Discussion started: 30 July 2024

where our study site is located. Starting in April, the area exhibiting stable and significant correlation begins to expand, encompassing Romania, the Republic of Moldova, the central part of Ukraine, and the eastern part of Bulgaria. From June onwards, the stable correlation extends to the eastern part of Europe and continues to increase, reaching its peak in August. During this month, the largest area is covered by stable and significant correlation, including the eastern and central parts of Europe (Figure 4). According to monthly correlation analyses and the stability map approach, we identified the August SPEI9 over the central and eastern parts of Europe (see the black square in Figure 4) as the most appropriate predictor for drought reconstruction.

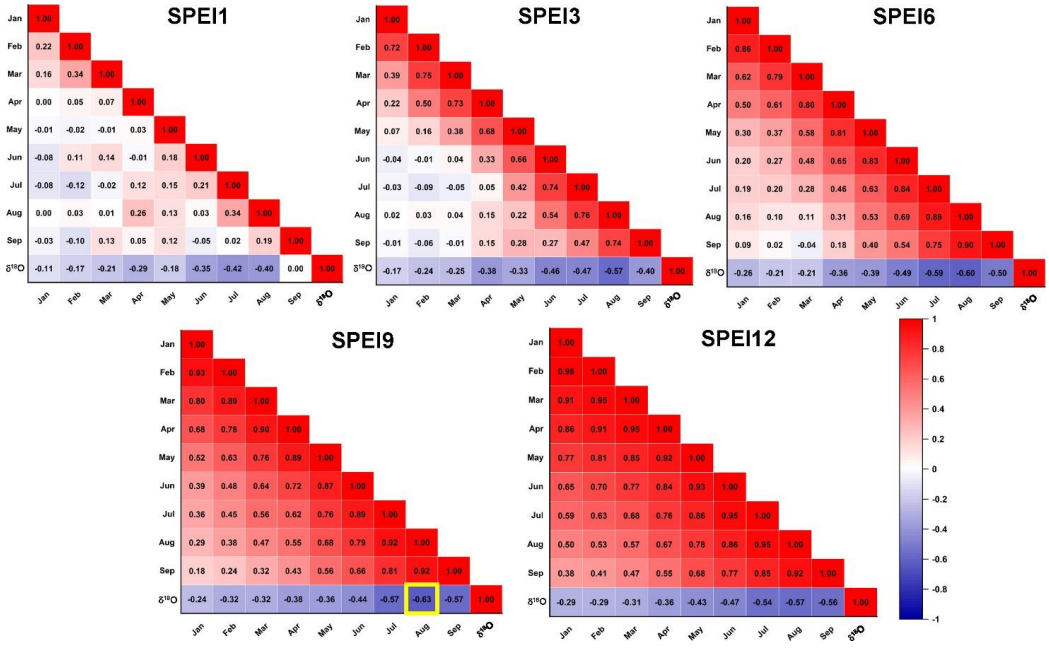

Figure 3. Correlation analyses between $\delta^{18}O$ values and SPEI drought index with different time windows a) SPEI1; b) SPEI3; c) SPEI6; d) SPEI9; e) SPEI12; from January to September, (95% significance level).

3.3 Drought reconstruction

In order to reconstruct the drought variability for the last 200 years, we used the August SPEI9 over the central and eastern parts of Europe (see the black square in Figure 4) as the predictand and the $\delta^{18}O$ chronology from the Letea Forest as the predictor. The reconstruction was developed using the linear regression model. Reconstruction skills were evaluated by splitting our chronology into two equally long periods, (1901 – 1960 and 1961 – 2020) for calibration – verification approach in forward and reverse mode (Figure 5). The calibration and verification models passed all the conventional verification tests, both in the forward and reverse modes. The positive values obtained for the reduction of error (RE) and coefficient of efficiency (CE) in forward and reverse mode (Table 1) indicate good and predictive reconstruction skills. These results are supported by a DW value near 2, which indicates low to no autocorrelation. Therefore, the obtained statistical results suggest that the linear regression model used is reliable, with high predictive skill for the August SPEI9 reconstruction over the central and eastern

https://doi.org/10.5194/egusphere-2024-2144
Preprint. Discussion started: 30 July 2024

parts of Europe. The developed reconstruction model can be used to reconstruct past long-term drought variability, it explains 40 % ($r^2 = 0.40$) of the drought variation over the analyzed region.

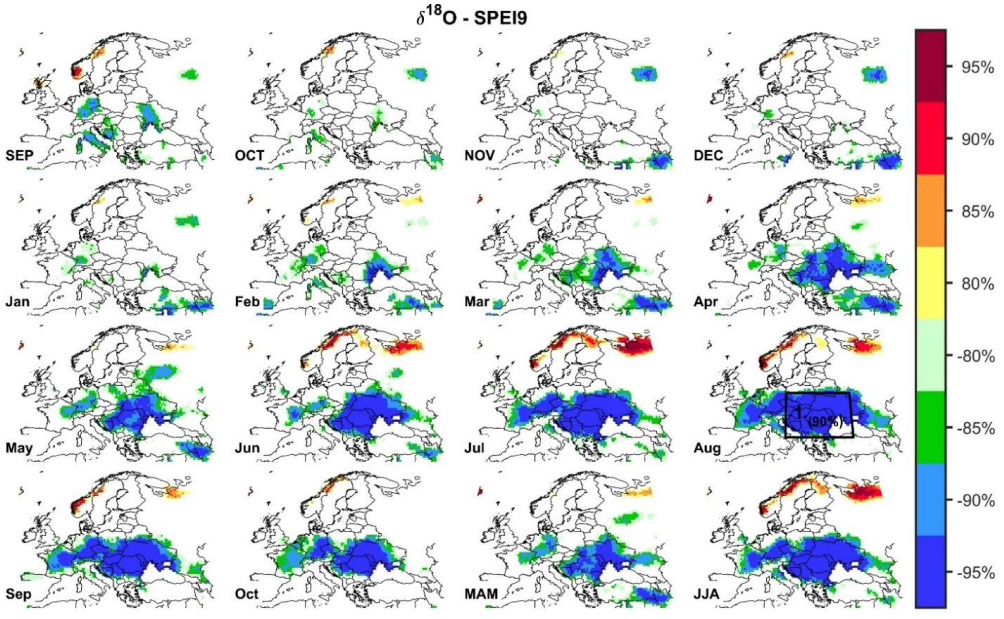

Figure 4. Stability map of the correlation between the $\delta^{18}O$ chorology and different monthly combinations of SPEI9 from the previous year September until the current year October, but also for March, April, May (MAM), and June, July, August (JJA) periods. Regions where the correlation is stable, positive, and significant for at least 80% of windows are shaded with dark red (95%), red (90%), orange (85%), and yellow (80%). The corresponding regions where the correlation is stable, but negative, are shaded with dark blue (95%), blue (90%), green (85%), and light green (80%). Analyzed period: 1902–2020. The significance level is computed based on a two-tailed t-test.

250

The inter-annual to inter-decadal variation of our August SPEI9 drought reconstruction for the period 1807 - 2020 is presented in Figure 6. The tree-ring reconstruction generally matches both the interannual and decadal variability of the observed August SPEI9 variability. According to our results, the wettest long-term periods occurred between 1905 – 1915, 1934 – 1944, 1951 – 1958, and 1980 – 1995. The driest periods occurred between 1818 – 1835, 1845 – 1854, 1882 – 1890,
255 and 2007 – 2020, maintaining the decreasing trend. Interestingly, the dry and wet periods are not evenly distributed across time. The most wet periods were recorded during the 20th century, while the long-term dry periods were recorded in the 19th and 21st centuries.

https://doi.org/10.5194/egusphere-2024-2144
Preprint. Discussion started: 30 July 2024

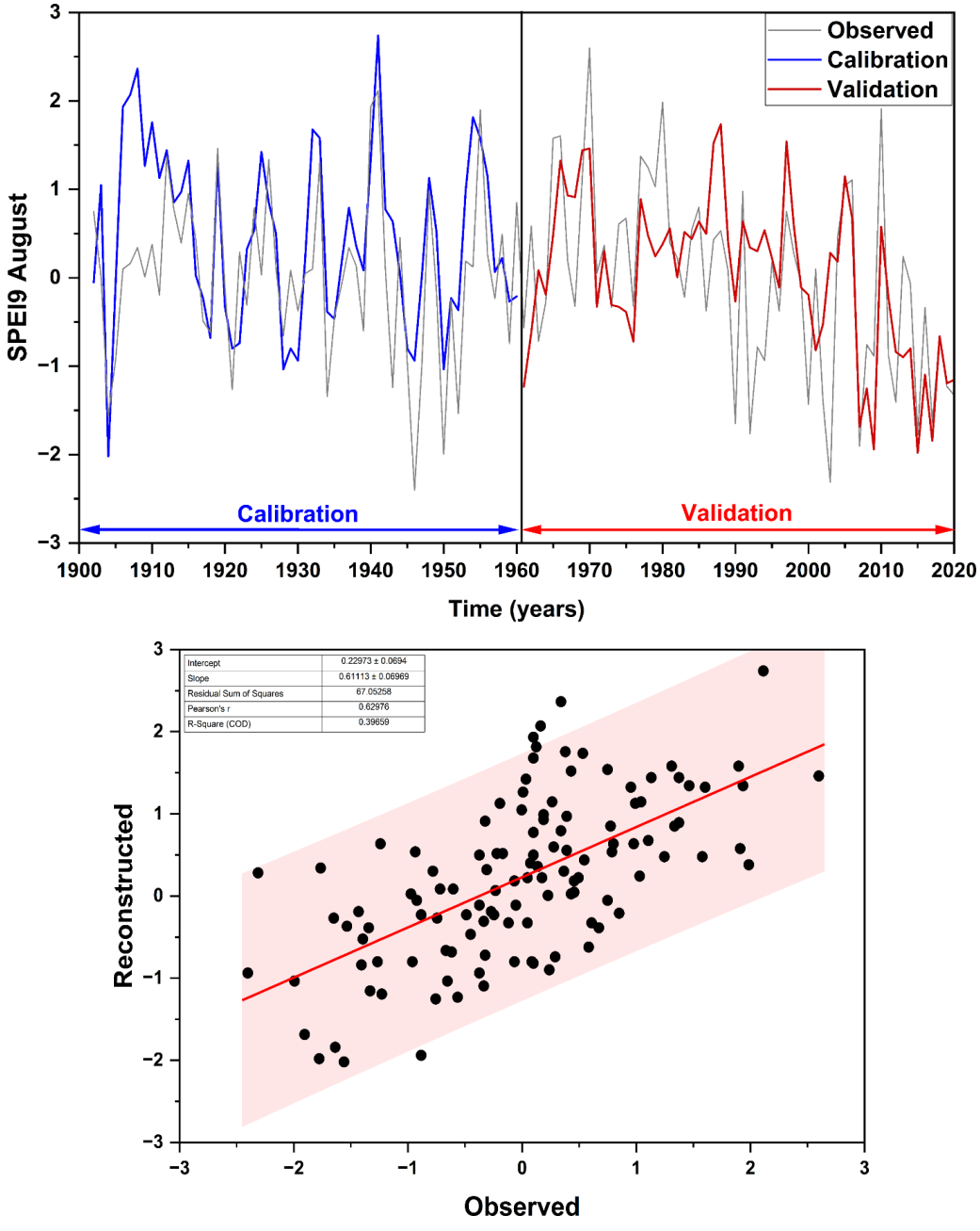

Figure 5. a) Calibration – validation model for the August SPEI9 reconstruction; in (a) the grey line indicates the observed data (CRU TS v. 4.04 dataset, Harris et al., 2020); the red line indicates the reconstructed August SPEI9 over the calibration period and the blue line indicates the reconstructed August SPEI9 over the validation period; and b) regression between the observed and reconstructed August SPEI9 over the period 1900 – 2020.

260 The extremes in the reconstructed August SPEI9 reconstruction, over the last 200 years were summarized by counting the number of years outside the 0.1 and 0.9 quantiles. Over the analyzed period we identified 31 extremely positive (wet) years

https://doi.org/10.5194/egusphere-2024-2144
Preprint. Discussion started: 30 July 2024

and 31 extremely negative (dry) years. The most extreme positive years are: 1954 and 1809 (1.82), 1906 (1.93), 1907 (2.07), 1908 (2.37), and 1941 (2.74) and the most extreme negative years are: 1873 (-2.10), 1834 (-2.16), 1833 (-2.20), 1822 (-2.20), 1863 (-2.86). The occurrence frequency of the extreme years corresponds with the distribution of the decadal variability. Only five extreme wet years were recorded in the 19th century and only four extreme dry years were recorded in the 20th century. The longest interval with continuous dry events is 10 years occurring between 2011 and 2020. Similarly, the maximum interval with continuous wet events was also 10 years occurring between 1906 and 1915.

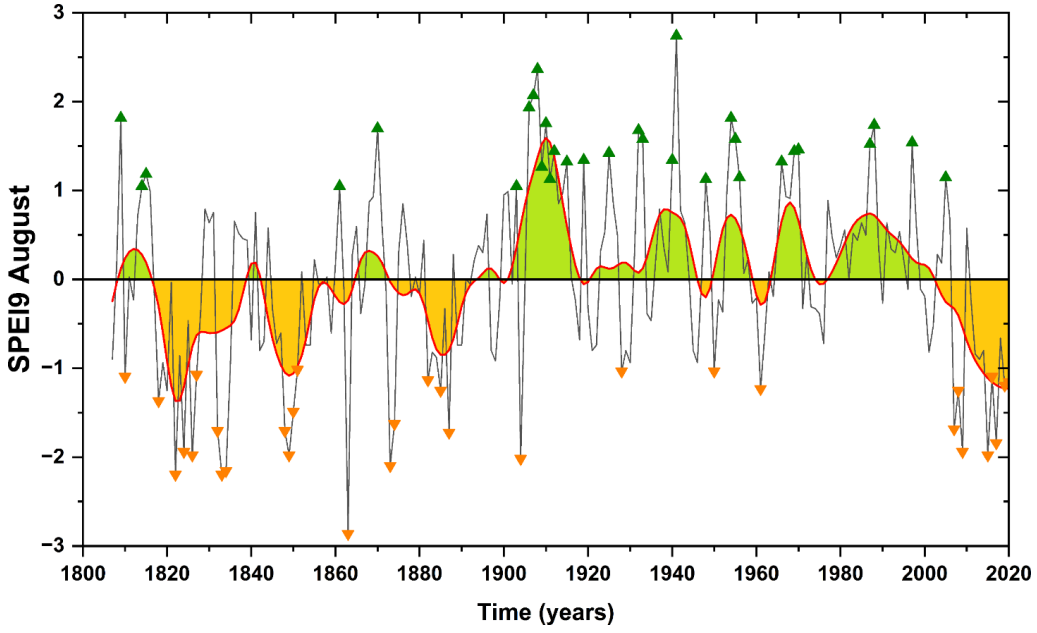

Figure 6. Reconstructed August SPEI9 (black line) for the 1800–2020 period, with a 31-year running mean (red line). Extreme dry/wet years are represented by lower-orange/upper-green triangles. Extreme years are defined as those in which the August SPEI9 index falls below −1.5 or exceeds +1.5 standard deviations.

3.4 $\delta^{18}O$ variability and large-scale atmospheric circulation

Previous studies have shown that the low- and high-frequency variability of $\delta^{18}O$ values in tree-ring cellulose over Europe is also influenced by the prevailing large scale-atmospheric circulation and the sea surface temperature (SST) (Ionita, 2015; Nagavciuc et al., 2019b; Roibu et al., 2022). Hence, we analyzed the influence of the large-scale atmospheric circulation on the variability $\delta^{18}O$ in tree-ring cellulose of Letea forest by computing composite maps for the years characterized by high $\delta^{18}O$ values (i.e., $\delta^{18}O > 1$ standard deviation) and low $\delta^{18}O$ values (i.e., $\delta^{18}O < -1$ standard deviation), respectively. Figure 7 shows that years with a high $\delta^{18}O$ value are associated with a high-pressure system over the North Atlantic Ocean extending towards the central and eastern part of Europe and a center of low-pressure anomalies south of Greenland. This type of large-scale structure over the central and southern parts of Europe suppresses ascending motions, and reduces water vapor condensation and precipitation formation. Consequently, this leads to drought conditions in the land surface areas beneath this system, including our study region (Figure 7a). This pattern is linked to Rossby-wave oscillation, as captured by the meridional wind at 200 mb and associated with high $\delta^{18}O$ values (Figure 7c). Shifts in the direction and intensity of meridional winds can contribute to the formation and persistence of blocking high-pressure systems. These systems act as barriers to the typical transport of moisture-laden air masses from the Atlantic or Mediterranean, hindering precipitation over eastern Europe. In

https://doi.org/10.5194/egusphere-2024-2144
Preprint. Discussion started: 30 July 2024

contrast, low values of $\delta^{18}O$ are associated with negative Z500 anomalies extending from the central Atlantic to Europe (Figure 7b). The center of negative Z500 anomalies over Europe is consistent with enhanced precipitation in our study region due to the advection of moisture from the Mediterranean and Black Seas (Figure 7b). Low $\delta^{18}O$ values are also associated with the prevalence of a hemispheric wave-4 pattern (Figure 7d), a pattern found to be linked with drought and heatwaves depending on the location of its centers of action (Yang et al., 2024).

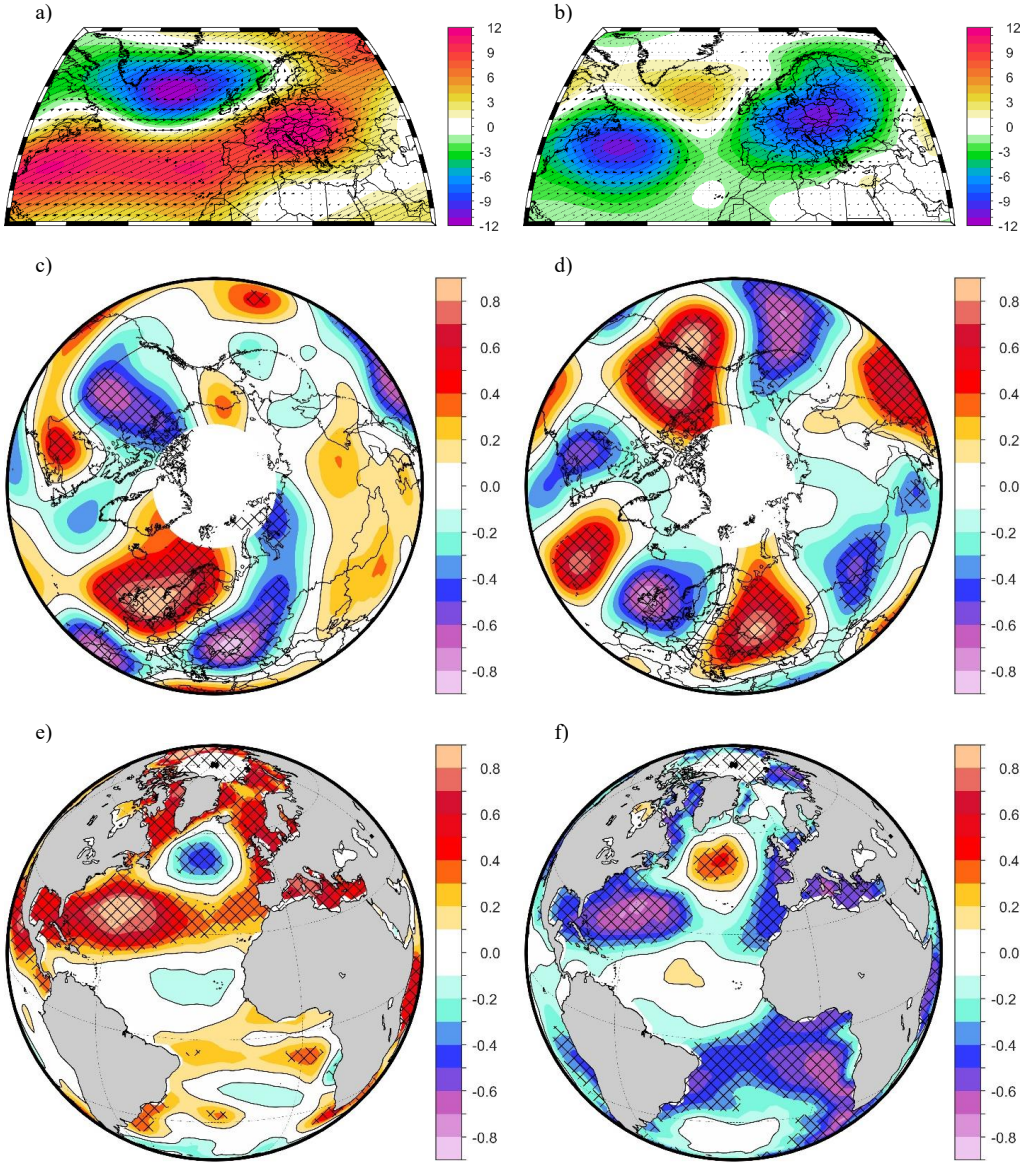

Figure 7. a) The composite map between high $\delta^{18}O$ values (> 1 std. dev.) and the annual (mean over the period December previous year until August current year) of geopotential height at 500 mb (Z500); b) the same as a) but for low $\delta^{18}O$ values (< −1 std. dev.); c) as in a) but for the meridional wind at 200mb (V200); d) as in b) but for the meridional wind at 200mb (V200); e) as in a) but for the sea surface temperature and f) as in b) but for the sea surface temperature. The hatching highlights significant correlation coefficients at a confidence level of 95%. Units: Z500 (m). Analyzed period: 1836–2020 for Z500 and V200 and 1855 – 2020 for the SST.

https://doi.org/10.5194/egusphere-2024-2144
Preprint. Discussion started: 30 July 2024

Similar large-scale structures have been found to be associated with $\delta^{18}O$ extreme values in the Calimani Mountains (Nagavciuc et al., 2020, 2022a). The $\delta^{18}O$ variability, both at the European level and more regionally, has been found to be influenced by the sea surface temperature anomalies, especially in the North Atlantic basin (Nagavciuc et al., 2024). In the current case, high values of $\delta^{18}O$ in tree-ring cellulose are associated with positive SST anomalies in the North Atlantic Ocean, the Mediterranean region, and the Black Sea and negative SST anomalies in the central Atlantic Ocean (Figure 7e). In contrast, low $\delta^{18}O$ values, correspond to negative SST anomalies over the Mediterranean Sea and the Black Sea and positive SST anomalies over the central Atlantic Ocean (Figure 7f). This particular SST pattern has been found to strongly affect the dry and wet conditions in the central and eastern parts of Europe, especially on decadal and multidecadal time scales, by influencing the prevailing large-scale atmospheric circulation (Ionita et al., 2022). Overall, in this section, we show that the combined impact of atmospheric and oceanic circulation is reflected in the $\delta^{18}O$ of tree rings from the eastern part of Europe. Disentangling the complex interplay of factors affecting the variability of $\delta^{18}O$ in tree ring cellulose is crucial for accurate climate reconstructions. Studies often integrate tree-ring data with climate models and other paleoclimate proxy data to gain a holistic understanding of past climate variations driven by shifts in atmospheric and oceanic circulation patterns.

3.5 Comparison with other records

Other dendroclimatic studies from eastern Europe indicate moisture sensitivity of the tree-ring parameters. To test the synchronicity of our reconstruction, we compared the obtained August SPEI9 reconstruction with four previously published reconstructions available in the surrounding area. We have selected two drought reconstructions: one August SPEI3 from the Eastern Carpathians, Romania (Nagavciuc et al., 2022a), and one September SPEI6 from the Czech Republic (Brázdil et al., 2016). Additionally, we included precipitation reconstruction from the eastern Black Sea Region, Turkey (Akkemik et al., 2005), and a streamflow reconstruction for the Lower Danube River, at Ceatal Izmail hydrometric station (Nagavciuc et al., 2023) (Figure 8). The results showed good synchronicity between analyzed reconstructions, maintaining both high and low-frequency variability similar to other reconstructions. The analyzed reconstructions present similar features of low frequency, with clear common characteristics that are coherent over a large spatial scale. For example, the low frequency of the reconstructed August SPEI9 in this study agrees with the summer drought Aug SPEI3 (Nagavciuc et al., 2022a) and Lower Danube streamflow (Nagavciuc et al., 2023).

A more detailed investigation of the selected reconstructions reveals a good agreement in high frequency variability, with significant correlations. The highest coefficient of correlation was obtained with the Aug SPEI3 reconstruction from Calimani Mountains, Romania ($r = 0.38$), likewise based on $\delta^{18}O$ in tree-ring cellulose. This is followed by the Lower Danube streamflow reconstruction based on tree-ring width from Caraorman Forest, Danube Delta, Romania ($r = 0.37$). Lower, but significant correlations were found with the September SPEI6 drought reconstruction in the Czech Republic ($r = 0.28$) from historical documents, and with the May-June precipitation record from the eastern Black Sea Region, Turkey ($r= 0.21$), derived from tree-ring width analysis.

Another important aspect regarding the similarities between analyzed reconstruction is the occurrence of the extreme events. We have identified a large number of extreme climate events in all five reconstructions, both positive (e.g. 1814, 1861, 1941, 1969, 1988) and negative (e.g. 1834, 1873, 1904, 1946, 1950, 2007, 2008, 2009). The occurrence of these extreme events is documented in numerous historical records. For example, in 1834 a severe drought was recorded in Moldova and Ardeal regions (Nagavciuc et al., 2022a; Pfister, 1999; Teodoreanu, 2017; Topor, 1963), also in Czech Lands (Brázdil et al., 2016, 2019). Additionally, a devastating drought occurred in central Turkey (Akkemik et al., 2005, 2008) during the same year. The year 1904 stands out in the records as a devastating drought event in Moldova and Romania (Nagavciuc et al., 2022a; Pfister, 1999; Teodoreanu, 2017; Topor, 1963), as well as in the Czech Lands (Brázdil et al., 2016, 2019). Furthermore, the years 1946,

https://doi.org/10.5194/egusphere-2024-2144
Preprint. Discussion started: 30 July 2024

2007, 2008, and 2009 are well known in the literature as extreme dry years. The wet events of our reconstruction are likewise mentioned in the documentary data. For example in 1814 was recorded as an extremely wet summer (Cernovodeanu and Binder, 1933; Pfister, 1999), not only in Romania, but also in Turkey (Akkemik et al., 2005, 2008). Another example, 1941 has been recognized as a very cold and rainy summer, with heavy rains (Nagavciuc et al., 2022a; Teodoreanu, 2017; Topor, 1963).

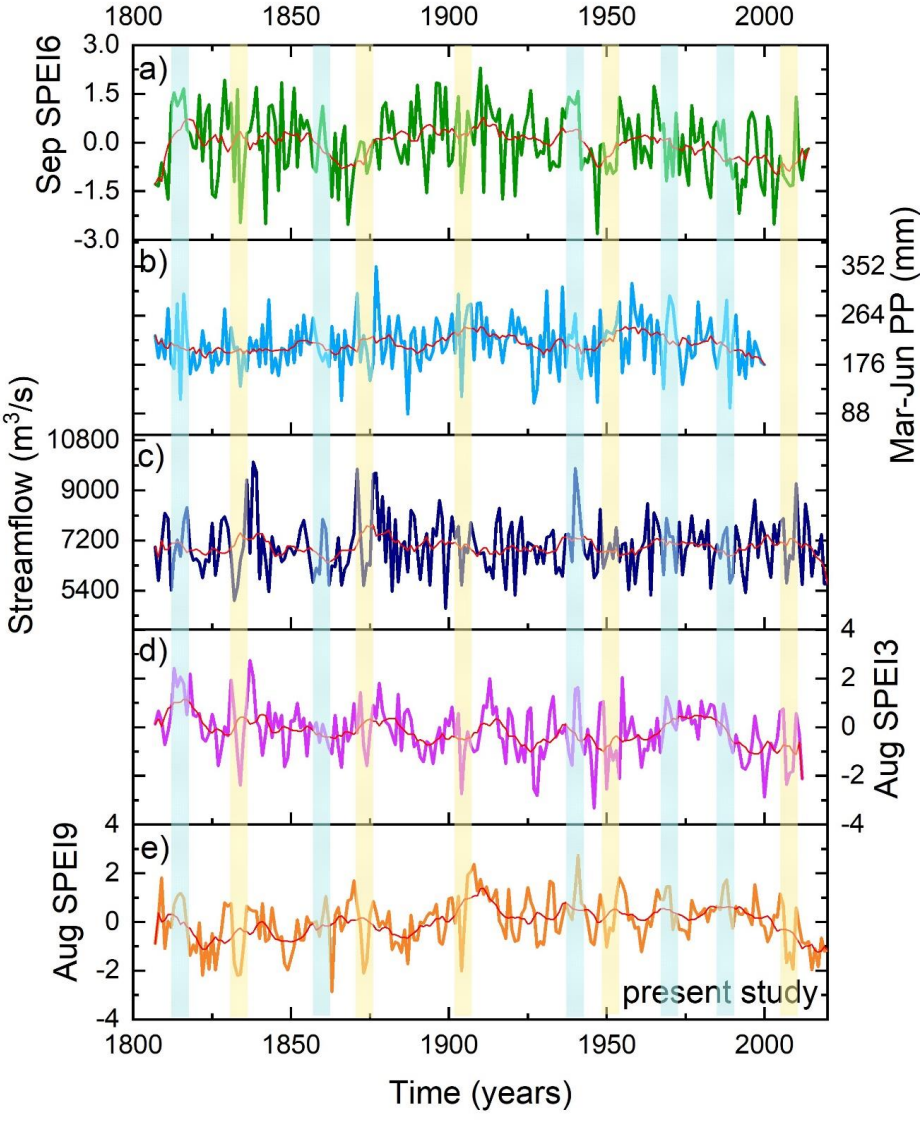

Figure 8. Comparison between different reconstructions a) September SPEI6 from Czech Republic (Brázdil et al., 2016); b) precipitation reconstruction from the eastern Black Sea Region, Turkey (Akkemik et al., 2005); c) streamflow reconstruction for Lower Danube River, at Ceatal Izmail hydrometric station (Nagavciuc et al., 2023); d) August SPEI3 from Eastern Carpathian, Romania (Nagavciuc et al., 2022a); e) August SPEI9 reconstruction (this study).

https://doi.org/10.5194/egusphere-2024-2144
Preprint. Discussion started: 30 July 2024

Thus, our reconstruction shows some clear common characteristics and patterns with the other reconstructions of droughts, pluvials, and streamflow and our comparison indicates that there is good agreement among the various reconstructions, despite differences in seasonality, used methodology and proxies, as well as site locations.

4. Conclusions

This study investigated the potential of $\delta^{18}O$ in oak tree ring cellulose from Letea Forest, Romania, as a proxy for reconstructing past drought variability. We developed a robust $\delta^{18}O$ chronology from the isotope time series of individual trees for the period 1803-2020CE. We found a significant negative correlation between $\delta^{18}O$ and various climatic parameters, including precipitation, relative humidity, and cloud cover. Conversely, $\delta^{18}O$ showed a positive correlation with temperature and sunshine duration. These relationships suggest that $\delta^{18}O$ primarily reflects moisture availability in the study area. Nevertheless, the strongest correlation was found between $\delta^{18}O$ and the Standardized Precipitation Evapotranspiration Index (SPEI9) for August over central and eastern Europe. This highlights the superior sensitivity of $\delta^{18}O$ to hydroclimatic conditions (August SPEI9), particularly on longer time scales, compared to relationships with temperature or precipitation data alone. The good regional relationship between August SPEI9 and $\delta^{18}O$ was confirmed by stability maps.

Using a linear regression model, we developed a reconstruction of August SPEI9 for the past 200 years based on the $\delta^{18}O$ chronology. The August SPEI9 drought reconstruction reveals valuable information on the interannual and decadal climate variability of the central-eastern part of Europe. According to our reconstruction, the wettest periods occurred during 1905-1915, 1934-1944, 1951-1958, and 1980-1995, the driest during 1818-1835, 1845-1854, 1882-1890, and 2007-2020. Interestingly, the most extreme wet periods occurred in the 20th century, while the most extreme dry periods were recorded in the 19th and 21st centuries.

Further analysis revealed that $\delta^{18}O$ variability is influenced by large-scale atmospheric circulation patterns. Years with high $\delta^{18}O$ values were associated with a high-pressure system over the North Atlantic, linked to Rossby-wave oscillations and positive sea surface temperature anomalies. Conversely, years with low $\delta^{18}O$ values corresponded to negative pressure anomalies over Europe, indicating enhanced precipitation. Additionally, sea surface temperature anomalies in the North Atlantic, Mediterranean, and Black Seas correspond to high and low $\delta^{18}O$ values, suggesting an interplay between atmospheric and oceanic circulation in influencing moisture availability over the analyzed region.

Comparison with other paleoclimate reconstructions from the region (drought, precipitation, and streamflow reconstructions) revealed good synchronicity and agreement in terms of both low and high-frequency variability, thus highlighting the robustness of our August SPEI9 reconstruction for central and eastern Europe.

Overall, this study demonstrates the valuable application of $\delta^{18}O$ in oak tree ring cellulose for reconstructing past hydroclimatic variability in the Letea Forest of the Danube River delta and central/eastern Europe. Combining tree-ring $\delta^{18}O$ records with other paleoclimate proxies and climate models can provide a more comprehensive understanding of long-term climate dynamics and their drivers. Future research can further refine drought reconstructions by incorporating additional environmental data and expanding the spatial coverage by studying additional tree sites.

https://doi.org/10.5194/egusphere-2024-2144
Preprint. Discussion started: 30 July 2024

Acknowledgements. V.N. and M.I. were partially supported by a grant of the Ministry of Research, Innovation and Digitization, under the "Romania's National Recovery and Resilience Plan – Founded by EU-NextGenerationEU" program, project "Compound extreme events from a long-term perspective and their impact on forest growth dynamics (CExForD)" number 760074/23.05.2023, code 287/30.11.2022, within Pillar III, Component C9, Investment 8. Monica Ionita was also supported by the Helmholtz Association through the joint program "Changing Earth - Sustaining our Future" (PoF IV) program of the AWI. and the Helmholtz Climate Initiative REKLIM.

Authors contributions. V.N. and M.I. designed the study and wrote the article draft. G.H., M.R., C-C.R, and M-G. C helped with the writing of the original draft, interpreting the results, and the review process.

Competing interests. The authors declare no competing interests.

Data availability. Data will be made available on request.

https://doi.org/10.5194/egusphere-2024-2144
Preprint. Discussion started: 30 July 2024

References

Abdelazim, M. N. and Diaconu, D. C., Eds.: The Danube River Delta, Earth and., Springer, Cham, Switzerland., 2022.

Administraţia Rezervaţiei Biosferei Delta Dunării: Conservarea Pădurii Caraorman, brandware.ro [online] Available from: https://brandware.ro/padurea-caraorman/conservare-padurea-caraorman/ (Accessed 11 January 2022), 2022.

Akkemik, Ü., Dağdeviren, N. and Aras, A.: A Preliminary Reconstruction (A.D. 1635-2000) of Spring Precipitation Using Oak Tree Rings in the Western Black Sea Region of Turkey, Int. J. Biometeorol., 49, 297–302, doi:10.1007/s00484-004-0249-8, 2005.

Akkemik, Ü., D'arrigo, R., Cherubini, P., Kose, N. and Jacoby, G. C.: Tree-ring reconstructions of precipitation and streamflow for north-western, Int. J. Climatol., 28, 173–183, 2008.

Allen, S. T., Kirchner, J. W., Braun, S., Siegwolf, R. T. W. and Goldsmith, G. R.: Seasonal origins of soil water used by trees, Hydrol. Earth Syst. Sci. Discuss., (November), 1–23, doi:10.5194/hess-2018-554, 2018.

Baker, J. C. A., Cintra, B. B. L., Gloor, M., Boom, A., Neill, D., Clerici, S., Leng, M. J., Helle, G. and Brienen, R. J. W.: The Changing Amazon Hydrological Cycle Inferences From Over 200 Years of Tree-Ring Oxygen isotope data, JGR Biogeosciences, 127, e2022JG006955, doi:10.1029/2022JG006955, 2022.

Brázdil, R., Dobrovolný, P., Trnka, M., Büntgen, U., Řezníčková, L., Kotyza, O., Valášek, H. and Štěpánek, P.: Documentary and instrumental-based drought indices for the Czech Lands back to AD 1501, Clim. Res., 70(2–3), 103–117, doi:10.3354/cr01380, 2016.

Brázdil, R., Dobrovolný, P., Trnka, M., Ř;ezníková, L., Dolák, L. and Kotyza, O.: Extreme droughts and human responses to them: The Czech Lands in the pre-instrumental period, Clim. Past, 15(1), 1–24, doi:10.5194/cp-15-1-2019, 2019.

Briffa, K. and Jones, P.: Basic chronology statistics and assessment, in Methods of dendrochronology, edited by E. Cook and L. Kairiukstis, pp. 137–152, Kluwer, Dordrecht., 1992.

Bunn, A. G.: A dendrochronology program library in R (dplR), Dendrochronologia, 26(2), 115–124, doi:http://dx.doi.org/10.1016/j.dendro.2008.01.002, 2008.

Cernovodeanu, P. and Binder, P.: Cavalerii Apocalipsilui Calamitățile naturale din trecutul României (până la 1800), SILEX-Casă de Editură, Presă și Impresarial S.R.L., Bucuresti., 1933.

Coplen, T. B.: Reporting of stable hydrogen, carbon, and oxygen isotopic abundances, Pure Appl. Chem., 66, 273–276, doi:10.1351/pac199466020273, 1994.

Cybis Elektronik: CDendro and CooRecorder. 2010. Available online: http://www.cybis.se/forfun/dendro/ index.htm., www.cybis.se [online] Available from: http://www.cybis.se/forfun/dendro/ index.htm (Accessed 12 January 2022), 2010.

Duffy, J. E., McCarroll, D., Loader, N. J., Young, G. H. F., Davies, D., Miles, D. and Bronk Ramsey, C.: Absence of Age-Related Trends in Stable Oxygen Isotope Ratios From Oak Tree Rings, Global Biogeochem. Cycles, 33(7), 841–848, doi:10.1029/2019GB006195, 2019.

Durbin, J. and Watson, G. S.: Testing for Serial Correlation in Least Squares Regression: I, Biometrika, 37(3/4), 409–428,

https://doi.org/10.5194/egusphere-2024-2144
Preprint. Discussion started: 30 July 2024

doi:10.2307/2332391, 1950.

Feng, X., Huang, R., Zhu, H., Liang, E., Bräuning, A., Zhong, L., Gong, Z., Zhang, P., Asad, F., Zhu, X. and Grießinger, J.: Tree-ring cellulose oxygen isotopes indicate atmospheric aridity in the western Kunlun Mountains, Ecol. Indic., 137, 108776, doi:10.1016/j.ecolind.2022.108776, 2022.

Freund, M. B., Helle, G., Balting, D. F., Ballis, N., Schleser, G. H. and Cubasch, U.: European tree-ring isotopes indicate unusual recent hydroclimate, Commun. Earth Environ., 4(1), 26, doi:10.1038/s43247-022-00648-7, 2023.

Gagen, M., Battipaglia, G., Daux, V., Duffy, J., Dorado-Liñán, I., Hayles, L. A., Martínez-Sancho, E., McCarroll, D., Shestakova, T. A. and Treydte, K.: Climate Signals in Stable Isotope Tree-Ring Records, in Stable Isotopes in Tree Rings. Tree Physiology, edited by R. T. W. Siegwolf, J. R. Brooks, J. Roden, and M. Saurer, pp. 537–579, Springer International Publishing, Cham., 2022.

Gärtner, H. and Nievergelt, D.: The core-microtome: A new tool for surface preparation on cores and time series analysis of varying cell parameters, Dendrochronologia, 28(2), 85–92, doi:https://doi.org/10.1016/j.dendro.2009.09.002, 2010.

Gessler, A., Ferrio, J. P., Hommel, R., Treydte, K., Werner, R. A. and Monson, R. K.: Stable isotopes in tree rings: Towards a mechanistic understanding of isotope fractionation and mixing processes from the leaves to the wood, Tree Physiol., 34(8), 796–818, doi:10.1093/treephys/tpu040, 2014.

Gessler, A., Bächli, L., Rouholahnejad Freund, E., Treydte, K., Schaub, M., Haeni, M., Weiler, M., Seeger, S., Marshall, J., Hug, C., Zweifel, R., Hagedorn, F., Rigling, A., Saurer, M. and Meusburger, K.: Drought reduces water uptake in beech from the drying topsoil, but no compensatory uptake occurs from deeper soil layers, New Phytol., 233(1), 194–206, doi:10.1111/nph.17767, 2022.

Harris, I., Osborn, T. J., Jones, P. and Lister, D.: Version 4 of the CRU TS monthly high-resolution gridded multivariate climate dataset, Sci. Data, 7(1), 1–18, doi:10.1038/s41597-020-0453-3, 2020.

Helle, G., Pauly, M., Heinrich, I., Schollän, K., Balanzategui, D. and Schürheck, L.: Stable Isotope Signatures of Wood, its Constituents and Methods of Cellulose Extraction, in Stable Isotopes in Tree Rings: Inferring Physiological, Climatic and Environmental Responses, edited by R. T. W. Siegwolf, J. R. Brooks, J. Roden, and M. Saurer, pp. 135–190, Springer International Publishing, Cham., 2022.

Holmes, R. L.: Computer-assisted quality control in tree-ring dating and measurement, Tree Ring Bull., 43, 69–75, 1983.

info-delta: Pădurea Letea, info-delta.ro [online] Available from: https://www.info-delta.ro/delta-dunarii-17/padurea-letea--120.html (Accessed 19 October 2023), 2023.

Ionita, M.: Interannual summer streamflow variability over Romania and its connection to large-scale atmospheric circulation, Int. J. Climatol., 35(14), 4186–4196, doi:10.1002/joc.4278, 2015.

Ionita, M. and Nagavciuc, V.: Changes in drought features at the European level over the last 120 years, Nat. Hazards Earth Syst. Sci., 21, 1685–1701, doi:10.5194/nhess-21-1685-2021, 2021.

Ionita, M., Lohmann, G. and Rimbu, N.: Prediction of spring Elbe discharge Based on stable teleconnections with winter global temperature and precipitation, J. Clim., 21(23), 6215–6226, doi:10.1175/2008JCLI2248.1, 2008.

https://doi.org/10.5194/egusphere-2024-2144
Preprint. Discussion started: 30 July 2024

Ionita, M., Dima, M., Lohmann, G., Scholz, P. and Rimbu, N.: Predicting the June 2013 European Flooding Based on Precipitation, Soil Moisture, and Sea Level Pressure, J. Hydrometeorol., 16(2), 598–614, doi:10.1175/JHM-D-14-0156.1, 2014.

Ionita, M., Scholz, P., Grosfeld, K. and Treffeisen, R.: Moisture transport and Antarctic sea ice: Austral spring 2016 event, Earth Syst. Dyn., 9, 939–954, doi:doi.org/10.5194/esd-9-939-2018, 2018.

Ionita, M., Caldarescu, D. E. and Nagavciuc, V.: Compound Hot and Dry Events in Europe: Variability and Large-Scale Drivers, Front. Clim., 3(June), 688991, doi:10.3389/fclim.2021.688991, 2021.

Ionita, M., Nagavciuc, V., Scholz, P. and Dima, M.: Long-term drought intensification over Europe driven by the weakening trend of the Atlantic Meridional Overturning Circulation, J. Hydrol. Reg. Stud., 42, 101176, doi:https://doi.org/10.1016/j.ejrh.2022.101176, 2022.

IPCC: Summary for policymakers, in Climate Change 2021: The Physical Science Basis. Contribution of Working Group I to the Sixth Assessment Report of the Intergovernmental Panel on Climate Change, edited by V. Masson-Delmotte, P. Zhai, A. Pirani, S. L. Connors, C. Péan, S. Berger, N. Caud, Y. Chen, L. Goldfarb, M. I. Gomis, M. Huang, K. Leitzell, E. Lonnoy, J. B. R. Matthews, T. K. Maycock, T. Waterfield, O. Yelekçi, R. Yu, and B. Zhou, pp. 3–22, Cambridge University Press, Cambridge, United Kingdom and New York, NY, USA., 2021.

Kreibich, H., Van Loon, A. F., Schröter, K., Ward, P. J., Mazzoleni, M., Sairam, N., Abeshu, G. W., Agafonova, S., AghaKouchak, A., Aksoy, H., Alvarez-Garreton, C., Aznar, B., Balkhi, L., Barendrecht, M. H., Biancamaria, S., Bos-Burgering, L., Bradley, C., Budiyono, Y., Buytaert, W., Capewell, L., Carlson, H., Cavus, Y., Couasnon, A., Coxon, G., Daliakopoulos, I., de Ruiter, M. C., Delus, C., Erfurt, M., Esposito, G., François, D., Frappart, F., Freer, J., Frolova, N., Gain, A. K., Grillakis, M., Grima, J. O., Guzmán, D. A., Huning, L. S., Ionita, M., Kharlamov, M., Khoi, D. N., Kieboom, N., Kireeva, M., Koutroulis, A., Lavado-Casimiro, W., Li, H.-Y., LLasat, M. C., Macdonald, D., Mård, J., Mathew-Richards, H., McKenzie, A., Mejia, A., Mendiondo, E. M., Mens, M., Mobini, S., Mohor, G. S., Nagavciuc, V., Ngo-Duc, T., Thao Nguyen Huynh, T., Nhi, P. T. T., Petrucci, O., Nguyen, H. Q., Quintana-Seguí, P., Razavi, S., Ridolfi, E., Riegel, J., Sadik, M. S., Savelli, E., Sazonov, A., Sharma, S., Sörensen, J., Arguello Souza, F. A., Stahl, K., Steinhausen, M., Stoelzle, M., Szalińska, W., Tang, Q., Tian, F., Tokarczyk, T., Tovar, C., Tran, T. V. T., Van Huijgevoort, M. H. J., van Vliet, M. T. H., Vorogushyn, S., Wagener, T., Wang, Y., Wendt, D. E., Wickham, E., Yang, L., Zambrano-Bigiarini, M., Blöschl, G. and Di Baldassarre, G.: The challenge of unprecedented floods and droughts in risk management, Nature, 608(7921), 80–86, doi:10.1038/s41586-022-04917-5, 2022.

Laumer, W., Andreu, L., Helle, G., Schleser, G. H., Wieloch, T. and Wissel, H.: A novel approach for the homogenization of cellulose to use micro-amounts for stable isotope analyses, Rapid Commun. Mass Spectrom., 23(13), 1934–1940, 2009.

Leavitt, S. W.: Tree-ring C–H–O isotope variability and sampling, Sci. Total Environ., 408(22), 5244–5253, doi:http://dx.doi.org/10.1016/j.scitotenv.2010.07.057, 2010.

Loader, N. J., Young, G. H. F., McCarroll, D., Davies, D., Miles, D. and Bronk Ramsey, C.: Summer precipitation for the England and Wales region, 1201–2000 CE, from stable oxygen isotopes in oak tree rings, J. Quat. Sci., 35(6), 731–736, doi:10.1002/jqs.3226, 2020.

Van Loon, A. F., Kchouk, S., Matanó, A., Tootoonchi, F., Alvarez-Garreton, C., Hassaballah, K. E. A., Wu, M., Wens, M. L. K., Shyrokaya, A., Ridolfi, E., Biella, R., Nagavciuc, V., Barendrecht, M. H., Bastos, A., Cavalcante, L., de Vries, F. T.,

https://doi.org/10.5194/egusphere-2024-2144
Preprint. Discussion started: 30 July 2024

Garcia, M., Mård, J., Streefkerk, I. N., Teutschbein, C., Tootoonchi, R., Weesie, R., Aich, V., Boisier, J. P., Di Baldassarre, G., Du, Y., Galleguillos, M., Garreaud, R., Ionita, M., Khatami, S., Koehler, J. K. L., Luce, C. H., Maskey, S., Mendoza, H. D., Mwangi, M. N., Pechlivanidis, I. G., Ribeiro Neto, G. G., Roy, T., Stefanski, R., Trambauer, P., Koebele, E. A., Vico, G. and Werner, M.: Review article: Drought as a continuum: memory effects in interlinked hydrological, ecological, and social systems, EGUsphere, 2024, 1–78, doi:10.5194/egusphere-2024-421, 2024.

McCarroll, D. and Loader, N. J.: Stable isotopes in tree rings, Quat. Sci. Rev., 23(7–8), 771–801, doi:http://dx.doi.org/10.1016/j.quascirev.2003.06.017, 2004.

Nagavciuc, V., Roibu, C., Ionita, M., Mursa, A., Cotos, M. and Popa, I.: Different climate response of three tree ring proxies of Pinus sylvestris from the Eastern Carpathians, Romania, Dendrochronologia, 54, 56–63, doi:10.1016/j.dendro.2019.02.007, 2019a.

Nagavciuc, V., Ionita, M., Perșoiu, A., Popa, I., Loader, N. J. and McCarroll, D.: Stable oxygen isotopes in Romanian oak tree rings record summer droughts and associated large-scale circulation patterns over Europe, Clim. Dyn., 52, 6557–6568, doi:doi.org/10.1007/s00382-018-4530-7, 2019b.

Nagavciuc, V., Kern, Z., Ionita, M., Hartl, C., Konter, O., Esper, J. and Popa, I.: Climate signals in carbon and oxygen isotope ratios of Pinus cembra tree-ring cellulose from Călimani Mountains, Romania, Int. J. Climatol., 40(5), 2539–2556, doi:10.1002/joc.6349, 2020.

Nagavciuc, V., Ionita, M., Kern, Z., McCarroll, D. and Popa, I.: A ~700 years perspective on the 21st century drying in the eastern part of Europe based on δ18O in tree ring cellulose, Commun. Earth Environ., 3, 277, doi:10.1038/s43247-022-00605-4, 2022a.

Nagavciuc, V., Scholz, P. and Ionita, M.: Hotspots for warm and dry summers in Romania, Nat. Hazards Earth Syst. Sci., 22(4), 1347–1369, doi:10.5194/nhess-22-1347-2022, 2022b.

Nagavciuc, V., Roibu, C.-C., Mursa, A., Știrbu, M.-I., Popa, I. and Ionita, M.: The first tree-ring reconstrruction of streamflow variability over the last ~250 years in the Lower Danube, J. Hydrol., 617, 129150, doi:10.1016/j.jhydrol.2023.129150, 2023.

Nagavciuc, V., Michel, S. L. L., Balting, D. F., Helle, G., Freund, M., Schleser, G. H., Steger, D. N., Lohmann, G. and Ionita, M.: A past and present perspective on the European summer vapor pressure deficit, Clim. Past, 20(3), 573–595, doi:10.5194/cp-20-573-2024, 2024.

Paul, D., Skrzypek, G. and Fórizs, I.: Normalization of measured stable isotopic compositions to isotope reference scales – a review, Rapid Commun. Mass Spectrom., 21, 3006–3014, doi:10.1002/rcm 10970231, 2007.

Pfister, C.: Wetternachhersage. 500 Jahre Klimavariationen und Naturkatastrophen (1496-1995), Verlag Paul Haupt, Bern Stuttgart Wien., 1999.

Pumijumnong, N., Bräuning, A., Sano, M., Nakatsuka, T., Muangsong, C. and Buajan, S.: A 338-year tree-ring oxygen isotope record from Thai teak captures the variations in the Asian summer monsoon system, Sci. Rep., 10, 8966, doi:10.1038/s41598-020-66001-0, 2020.

Robertson, I., Field, E. M., Heaton, T. H. E., Pilcher, J. R., Pollard, A.M. Switsur, V.R. Waterhouse, J.S. Frenzel, B., Stauffer,

https://doi.org/10.5194/egusphere-2024-2144
Preprint. Discussion started: 30 July 2024

B. and Weiss, M. M.: Problems of stable isotopes in tree-rings, lake sediments and peat-bogs as climatic evidence for the Holocene, Paläoklima., European Science Foundation, Strasbourg., 1995.

Roden, J., Lin, G. and Ehleringer, J. R.: A mechanistic model for interpretation of hydrogen and oxygen isotope ratios in tree-ring cellulose, Geochim. Cosmochim. Acta, 64(1), 21–35, 2000.

Roibu, C.-C., Nagavciuc, V., Ionita, M., Popa, I., Horodnic, S.-A., Mursa, A. and Büntgen, U.: A tree ring-based hydroclimate reconstruction for eastern Europe reveals large-scale teleconnection patterns, Clim. Dyn., (0123456789), doi:10.1007/s00382-022-06255-8, 2022.

Saurer, M., Kress, A., Leuenberger, M., Rinne, K. T., Treydte, K. S. and Siegwolf, R. T. W.: Influence of atmospheric circulation patterns on the oxygen isotope ratio of tree rings in the Alpine region, J. Geophys. Res. Atmos., 117(5), D05118, doi:10.1029/2011JD016861, 2012.

Schweingruber, F. H.: Tree Rings Basics and Applications of Dendrochronology., 1988.

Siegwolf, R. T. W., Brooks, J. R., Roden, J. and Saurer, M., Eds.: Stable Isotopes in Tree Rings Inferring Physiological, Climatic and Environmental Responses, Series Tit., Springer, Cham, Switzerland., 2022.

Van der Sleen, P., Groenendijk, P. and Zuidema, P. A.: Tree-ring δ18O in African mahogany (Entandrophragma utile) records regional precipitation and can be used for climate reconstructions, Glob. Planet. Change, 127, 58–66, doi:10.1016/j.gloplacha.2015.01.014, 2015.

Teodoreanu, E.: În căutarea timpului trecut Schiță de climatologie istorică, Editura Paodeia, Bucuresti., 2017.

Topor, N.: Anii ploioşi şi secetoşi din Republica Populară Romînă, C.S.A Institutul Meteorologic, Bucureşti., 1963.

Yang, X., Zeng, G., Zhang, S., Iyakaremye, V., Shen, C., Wang, W.-C. and Chen, D.: Phase-Locked Rossby Wave-4 Pattern Dominates the 2022-Like Concurrent Heat Extremes Across the Northern Hemisphere, Geophys. Res. Lett., 51(4), e2023GL107106, doi:https://doi.org/10.1029/2023GL107106, 2024.

Young, G. H. F., Loader, N. J., McCarroll, D., Bale, R. J., Demmler, J. C., Miles, D., Nayling, N. T., Rinne, K. T., Robertson, I., Watts, C. and Whitney, M.: Oxygen stable isotope ratios from British oak tree-rings provide a strong and consistent record of past changes in summer rainfall, Clim. Dyn., 45(11), 3609–3622, doi:10.1007/s00382-015-2559-4, 2015.

Zang, C. and Biondi, F.: Treeclim: An R package for the numerical calibration of proxy-climate relationships, Ecography (Cop.)., 38(4), 431–436, doi:10.1111/ecog.01335, 2015.

https://doi.org/10.5194/egusphere-2024-2144
Preprint. Discussion started: 30 July 2024

Table 1. Reconstruction skills table of calibration and verification statistics of the August SPEI9 based on the $\delta^{18}O$ values from Letea Forest, Analyzed period 1901 – 2020. the correlation coefficient (r), the coefficient of determination (r^2), the reduction of error (RE), and the coefficient of efficiency (CE).

Subsets lengths	r	r^2	RE	CE	DW
Early calibration (1901–1960)/late verification (1961–2020)	**-0.67**	**0.45**	**0.34**	**0.34**	**1.96**
Early verification (1901–1960)/late calibration (1961–2020)	**-0.62**	**0.38**	**0.35**	**0.35**	**1.64**
Full calibration period (1922–2013)	**-0.63**	**0.40**			

A long-term drought reconstruction based on oxygen isotope tree ring data

Viorica Nagavciuc [1,2*] Gerhard Helle [3], Maria Rădoane [2], Cătălin-Constantin Roibu [2], Mihai-Gabriel Cotos [2] and Monica Ionita[1,2*]

[1] Alfred Wegener Institute for Polar and Marine Research, Bremerhaven 27570, Germany

[2] Forest Biometrics Laboratory – Faculty of Forestry, "Stefan cel Mare" University of Suceava, Universității Street No. 13, Suceava 720229, Romania

[3] German Research Centre for Geosciences GFZ, 4.3 Climate Dynamics and Landscape Evolution, Telegrafenberg, 14473 Potsdam, Germany

**Correspondence to*: Monica Ionita (Monica.Ionita@awi.de); Viorica Nagavciuc (nagavciuc.viorica@gmail.com);

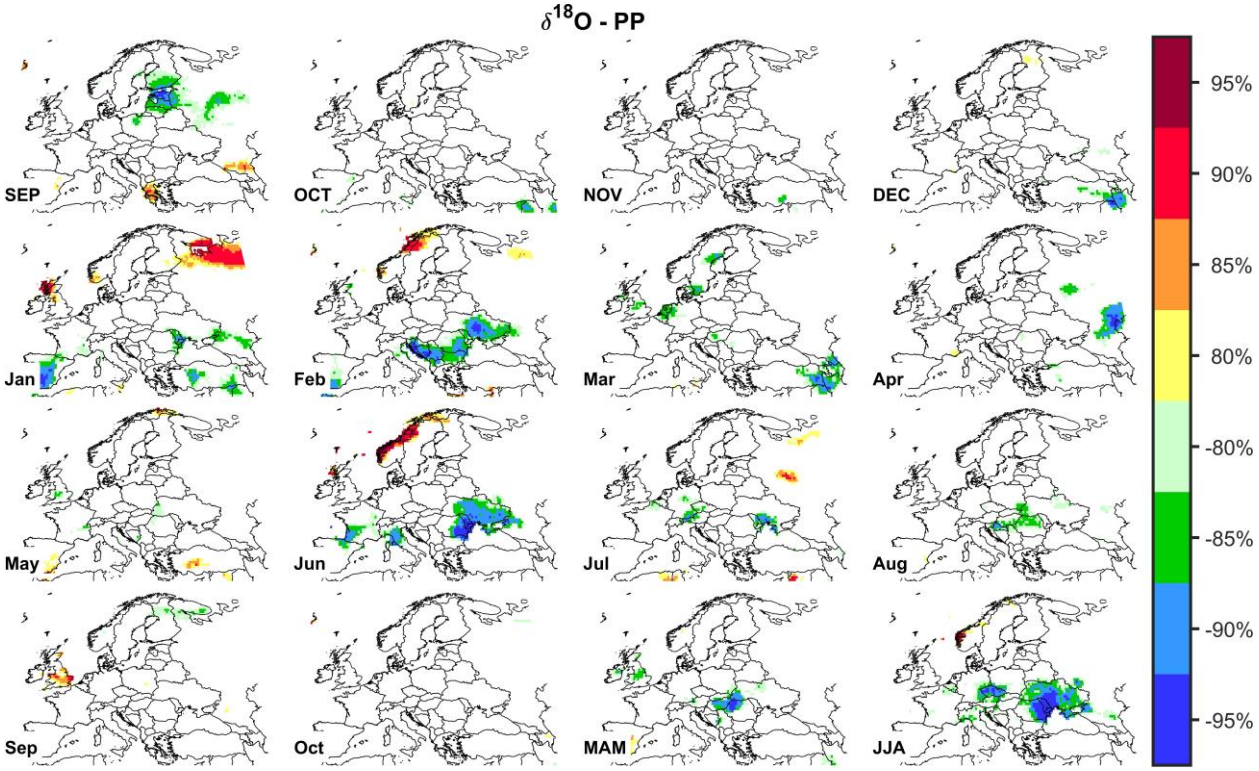

Figure S1. Stability map of the correlation between the $\delta^{18}O$ chorology and different monthly combinations of precipitation from the previous year September until the current year October, but also for March, April, May (MAM), and June, July, August (JJA) periods. Regions where the correlation is stable, positive, and significant for at least 80% windows are shaded with dark red (95%), red (90%), orange (85%), and yellow (80%). The corresponding regions where the correlation is stable, but negative, are shaded with dark blue (95%), blue (90%), green (85%), and light green (80%). Analyzed period: 1902–2020. The significance level is computed based on a two-tailed t-test.

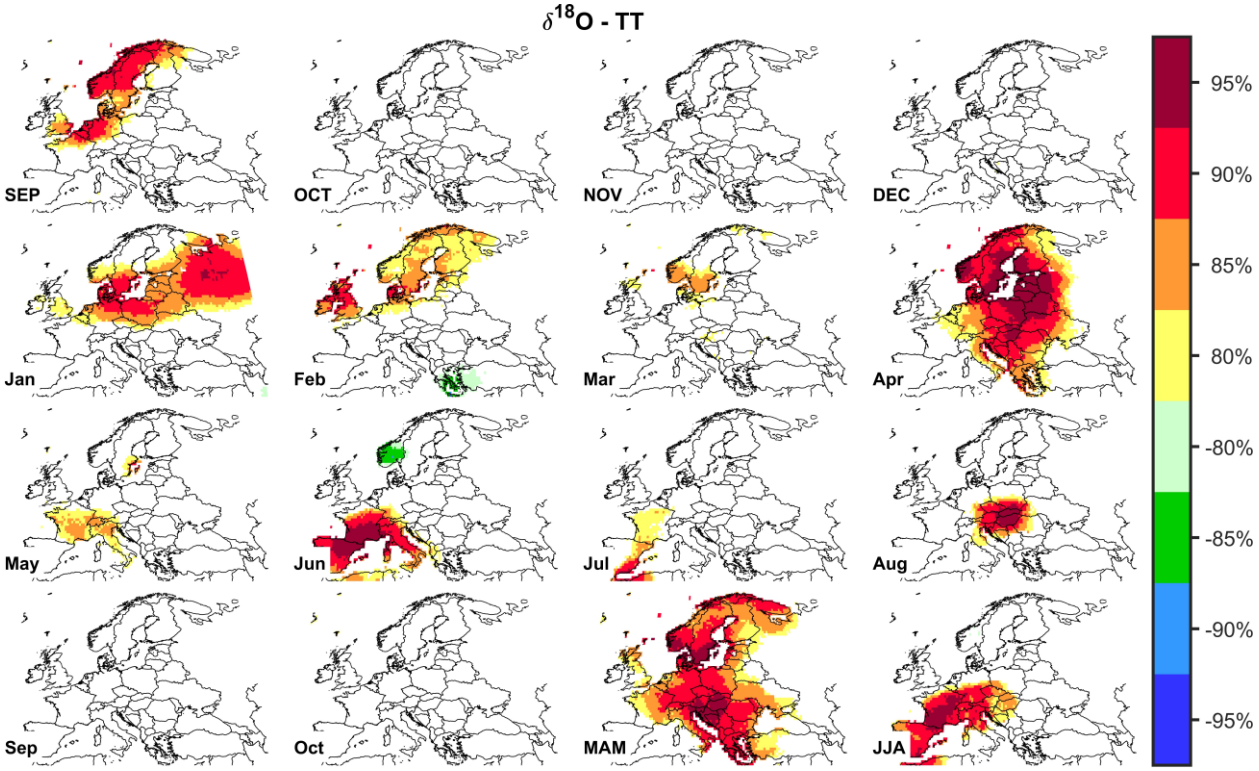

Figure S2. Stability map of the correlation between the $\delta^{18}O$ chorology and different monthly combinations of mean temperature from the previous year September until the current year October, but also for March, April, May (MAM), and June, July, August (JJA) periods. Regions where the correlation is stable, positive, and significant for at least 80% windows are shaded with dark red (95%), red (90%), orange (85%), and yellow (80%). The corresponding regions where the correlation is stable, but negative, are shaded with dark blue (95%), blue (90%), green (85%), and light green (80%). Analyzed period: 1902–2020. The significance level is computed based on a two-tailed t-test.

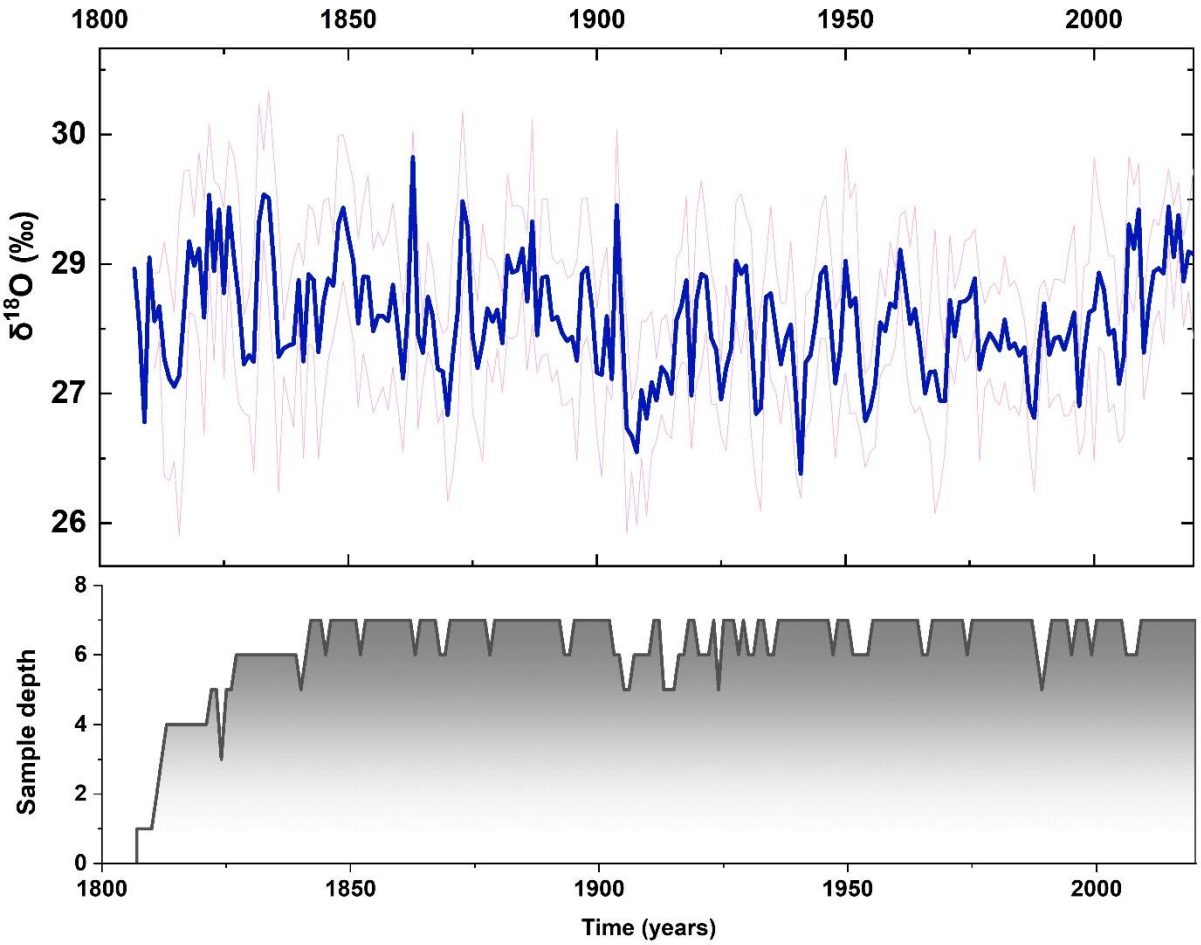

Figure S3. The master chronology of the $\delta^{18}O$ from the Letea Forest, Romania and the sample depth